

Cite this: DOI: 10.1039/c0xx00000x

www.rsc.org/xxxxxx

ARTICLE TYPE

# Rapid Diagnosis and Effective Inhibition of Corona Virus Using Spike Antibody Attached Gold Nanoparticle

Avijit Pramanik<sup>1</sup>, Ye Gao<sup>1</sup>, Shamily Patibandla<sup>1</sup>, Dipanwita Mitra<sup>2</sup>, Martin G. McCandless<sup>2</sup>,  
Lauren A Fassero<sup>2</sup>, Kalein Gates<sup>1</sup>, Ritesh Tandon<sup>2</sup>, and Paresh Chandra Ray<sup>1</sup> \*

Received (in XXX, XXX) Xth XXXXXXXXX 20XX, Accepted Xth XXXXXXXXX 20XX

DOI: 10.1039/b000000x

Severe acute respiratory syndrome coronavirus 2 (SARS-CoV-2) caused the coronavirus disease of 2019 (COVID-19) is responsible for 1.4 million death worldwide till now. Since no vaccine is yet available, a rapid diagnosis assay is very urgent for the society. Herein, we present the development of anti-spike antibody attached gold nanoparticle for rapid diagnosis of specific COVID-19 viral antigen or virus via simple colorimetric change observation within 5 minutes time period. For rapid and highly sensitive identification, surface enhanced Raman spectroscopy (SERS) has been employed using 4-amino thiophenol as reporter molecules, which are attached on gold nanoparticle via Au-S bond. In the presence of COVID-19 antigen or virus particles, due to the antigen-antibody interaction, gold nanoparticles undergo aggregation changing the color from pink to blue, which allows the determination of the presence of antigen or virus very rapidly through naked eye even at the concentration of 1 nano gram (ng)/mL for COVID-19 antigen and 1000 virus particles/mL for SARS-CoV-2 spike protein pseudotyped baculovirus. Importantly the aggregated gold nanoparticles forms several "hot spots" to provide very strong SERS signal enhancement from anti-spike antibody and 4-aminothiophenol attached gold nanoparticle via light-matter interactions. Finite-difference time-domain (FDTD) simulation data indicate that 4 orders of magnitude Raman enhancement in "hot spot" position, when gold nanoparticles formed aggregates. Using portable Raman analyzer, reported data demonstrate that antibody and 4-aminothiophenol attached gold nanoparticle-based SERS probe has the capability to detect COVID-19 antigen even at the concentration of 4 pico gram (pg)/mL and virus at the concentration of 18 virus particles/mL within 5 minutes of time period. Using HEK293T cells which express angiotensin-converting enzyme 2 (ACE2) by which SARS-CoV-2 enters human cells, we show that anti-spike antibody attached gold nanoparticle have the capability to inhibit the virus infection. Reported data show that antibody attached gold nanoparticles bind to SARS-CoV-2 spike protein, thereby inhibiting the virus from binding to the cell receptor, which stops virus infection and spread. It also has the capability to destroy the lipid membrane of the virus.

<sup>1</sup>Department of Chemistry and Biochemistry, Jackson State University, Jackson, MS, 39217, USA; E-mail: paresh.c.ray@jsums.edu;

<sup>2</sup>Department: Microbiology and Immunology, University of Mississippi Medical Center, Jackson, MS, 39216, USA

## Introduction

The outbreak of severe acute respiratory syndrome coronavirus-2 (SARS-CoV-2), also known as coronavirus disease of 2019 (COVID-19), is responsible for huge global disruption to health and economy<sup>1-10</sup>. As of November 13th, more than 59.4 million peoples have suffered by COVID-19 disease and around 1.40 million have died worldwide<sup>1-2</sup>. It is now well documented that spike (S), envelope (E), membrane (M), and nucleocapsid (N) are the important structural proteins for coronavirus particles<sup>6-16</sup>. Several reported data indicate that spike protein plays the most important role for virus entry and disease pathogenesis<sup>3-14</sup>. Since currently we do not have any FDA approved vaccine or therapeutic for the treatment of COVID-19 disease, rapid diagnosis is the key to slow the spread of COVID-19 and to save the lives<sup>1-20</sup>. Driven by the urgent need, we report the development of anti-spike antibody attached gold nanoparticle for rapid diagnosis of specific COVID-19 viral antigen (COVID-19 Spike Recombinant Antigen) or virus itself via naked eye colorimetric change and highly sensitive surface enhanced Raman spectroscopy (SERS). Recently, Ventura et al. have reported three different (spike, envelope, and membrane) antibodies attached GNP based colorimetric assay for highly sensitive COVID-19 detection<sup>14</sup>. In the current manuscript, we show that anti-spike antibody attached GNP has capability for ultrasensitive identification and well as inhibition of virus particles.

As we and others have reported before, due to good biocompatibility, size dependent optical properties and ease of modification of the surface, gold nanoparticle can be used for the development of excellent biosensing platform<sup>17-33</sup>. As shown in Figures S1 and S2 in the supporting information, the color of our anti-spike antibody attached gold nanoparticle is pink and it changed to bluish tinge in the presence of the COVID-19 antigen or virus due to the aggregation via antigen-antibody interaction. As a result, we observed color change upon aggregation. Based on the color observation with the naked eye, we can detect COVID-19 antigen even at the concentration of 1 nano gram (ng)/mL and virus particle at the concentration of 1000 virus particles/mL. Since SARS-CoV-2 is a biosafety-level-3 (BSL-3) virus, we have used a BSL-2, SARS-CoV-2 spike protein pseudotyped baculovirus (Pseudo SARS-CoV-2), as a model system for our diagnosis and inhibition experiment<sup>36-37</sup>.

Due to its extremely high sensitivity, SERS can be used for very low level of detection of virus, bacteria, cancer cells and different biomolecules<sup>17-27</sup>. It is now well documented that Raman signals can be enhanced by several orders ( $10^7$ - $10^{10}$ ) of magnitude by using plasmonic nanoparticle *via* the electromagnetic mechanism (EM) and chemical mechanism (CM)<sup>17-27</sup>. For rapid and highly sensitive identification, SERS has been employed using 4- amino thiophenol (4-ATP) as reporter molecules, which are attached to gold nanoparticle via Au-S bond. In the presence of COVID-19 antigen or virus particle, the aggregated nanoparticles form several “hot spots”. As we and other groups have reported that “hot spot” formation is a very important factor to provide extraordinary enhancements in SERS<sup>17-27</sup>, in the presence of COVID-19 antigen or virus particle strong SERS signals from 4-aminothiophenol have been observed, which allows to diagnose viral antigen even at the concentration of 4 pico gram (pg)/mL or virus at 18 virus particles/mL concentration.

It is now well documented that for SARS-CoV-2, the viral infections start with the binding of viral particles to receptors on the host cells, which is mediated by the spike protein<sup>8-17,34-41</sup>. As different study indicates that spike protein binds specifically to the human angiotensin-converting enzyme 2 (ACE2) receptor on the surface of human cells<sup>8-17</sup>, scientists from several groups are developing inhibitors which have the capability to block the mechanism by which the virus binds to the ACE2 receptor<sup>34-41</sup>. Herein, we demonstrate that anti-spike antibody attached gold nanoparticle has the capability to block the viral entry into cells using Pseudo SARS-CoV-2 as the model virus. Pseudo SARS-CoV-2 is BSL-1 baculoviruses pseudo typed with Spike (S) proteins. Using HEK293T cells which expresses ACE2 by which SARS-CoV-2 entry in human cells, we demonstrate that anti-spike antibody attached gold nanoparticle blocks viral replication and virus spread in HEK293T cells.

## Experimental Section

### Citrate coated gold Nanoparticle Synthesis

As shown in Figure S1A in the supporting information, citrate coated gold nanoparticles (GNP) were synthesized using HAuCl<sub>4</sub>, 3H<sub>2</sub>O and sodium citrate, as we and others have reported before<sup>17-30</sup>. For this purpose, we have used 0.01 % solution of HAuCl<sub>4</sub>, 3H<sub>2</sub>O and 1 wt % of sodium citrate. Transmission electron microscope (TEM), colorimetric study and dynamic light scattering (DLS) data have been used to characterize freshly synthesized nanoparticle. Table 1 shows the DLS data which indicate that the size of freshly prepared citrate coated GNP is  $\sim 15 \pm 2$  nm. Inserted picture in Figure S1A shows the color of freshly prepared GNPs are pink. As we and others have reported before, GNPs exhibits unique optical properties which are due to the surface plasmon resonance (SPR)<sup>17-30</sup>. It is well documented that the SPR band for citrate coated gold nanoparticles are due to the phase changes resulting from the increased rate of electron-surface collisions compared to larger particles<sup>28-33</sup>. Figure 1A shows the absorption spectra of citrate coated gold nanoparticle, which shows that  $\lambda_{max}$  for citrate coated gold nanoparticle is  $\sim 520$  nm. As we and others have reported before<sup>20-33</sup>, SPR of gold nanoparticles yield exceptionally high absorption with extinction coefficient  $\epsilon_{(15) 520nm} = 3.6 \times 10^8 \text{ cm}^{-1} \text{ M}^{-1}$ , which has been used here for sensing of COVID-19 antigen or virus using naked eye colorimetric study.

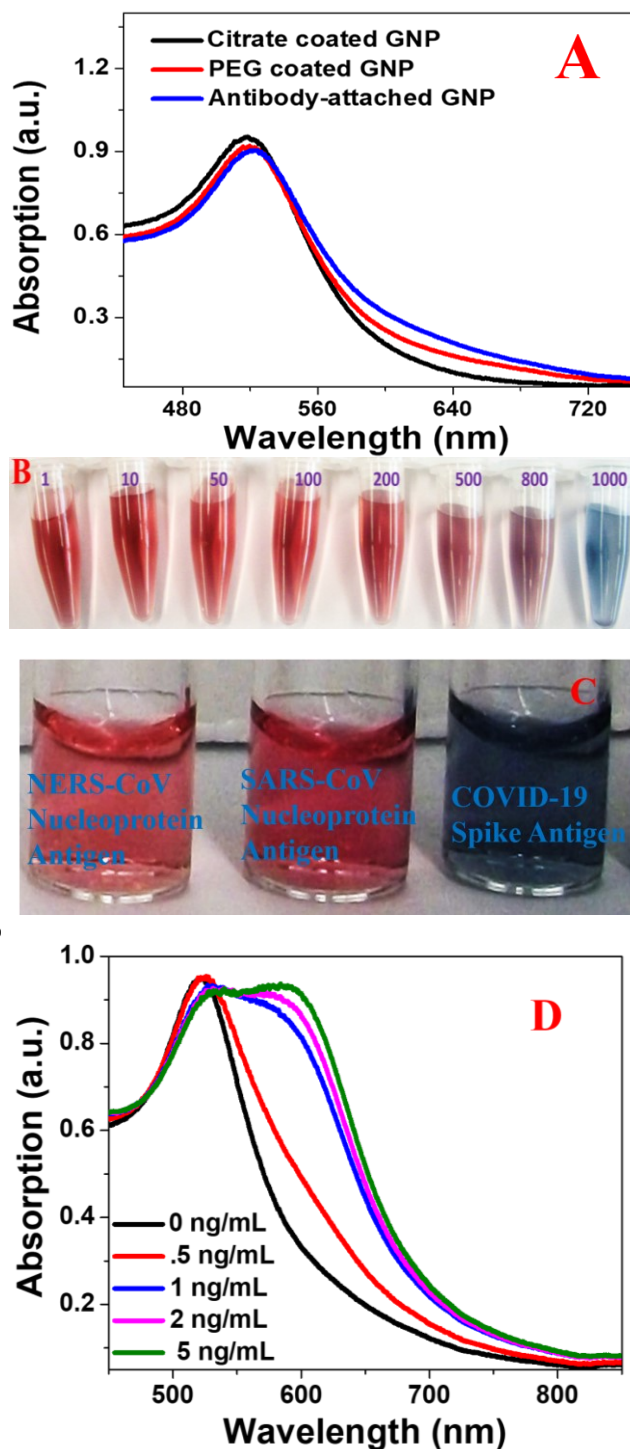


Figure 1: A) Absorption spectra from citrate coated gold nanoparticle, PEG coated gold nanoparticle and anti-spike antibody attached gold nanoparticle. B) Picture shows how the color of antibody attached GNPs in the presence of different amount of COVID-19 antigen from 1 pg/mL to 1000 pg/mL. C) Picture shows selectivity of anti-spike antibody attached gold nanoparticle based colorimetric assay for COVID-19 antigen (5 ng/mL). No color changes were observed in the presence of 5 ng/mL MERS-CoV nucleoprotein antigen and 5 ng/mL SERS-CoV nucleoprotein

**antigen. D) Figure shows how absorption spectra from antibody attached GNPs in the presence of different concentration COVID-19 antigen.**

The X-Ray diffraction (XRD) spectra from citrate coated gold nanoparticle as reported in Figure S2D shows the (111), (200), (220) and (311) diffraction peaks which are due to the face centered cubic gold (JCPDS 04-0784) <sup>20-30</sup>. The particle concentration was measured by UV-visible spectroscopy using the molar extinction coefficients at the wavelength of the maximum absorption of each gold colloid, [ $\epsilon_{(15)}^{519\text{nm}} = 3.6 \times 10^8 \text{ cm}^{-1} \text{ M}^{-1}$ ], as we and others reported before <sup>28-30</sup>.

### PEG coated gold Nanoparticle Synthesis

In the next step, as shown in Figure S1B in the supporting information, for developing biocompatible GNP, nanoparticles were coated with SH-PEG-CO<sub>2</sub>H. For developing biocompatible GNP, nanoparticles were coated with SH-PEG-CO<sub>2</sub>H. For this purpose, we have used Carboxy-PEG<sub>12</sub>-Thiol, (HS-PEG<sub>12</sub>-COOH). For this purpose, we have dissolved 10 mg HS-PEG<sub>12</sub>-COOH in 5 mL water and then added to citrate coated GNP using a syringe under vigorous stirring. After sonication the mixture for 30 minutes, the final products were separated through centrifugation. As reported in Table 1, after PEG coated the size of GNP increased to  $\sim 18 \pm 4$  nm. Inserted picture in Figure S1B shows the color of freshly prepared PEG coated GNPs are pink. Figure 1A shows the absorption spectra of PEG coated gold nanoparticle, which shows  $\lambda_{\text{max}}$  for PEG coated gold nanoparticle is  $\sim 521$  nm which indicates that after coating with PEG, the optical spectra for GNPs remains almost the same.

### Anti-spike-antibody coated gold Nanoparticle Synthesis

For targeted diagnosis and inhibition, we have developed anti-spike antibody attached gold nanoparticle. For this purpose, we have used EDC (1-ethyl-3-(3-dimethylaminopropyl)-carbodiimide)/NHS (N-hydroxysuccinimide) chemistry has been used. In short, we have added 0.2 molar (M) EDC and 0.05 M N-hydroxysulfosuccinimide sodium salt [1:3 (v/v) ratio] with the mixture of solution containing GNP and anti-spike antibody and the mixture was sonicated for 30 minutes. After that anti-spike antibody attached GNPs were separated from GNPs without antibody via centrifugation for 15 minutes at 6000 rpm, followed by resuspended in buffer. As reported in Table 1, after antibody attached the size of GNP increased to  $\sim 27 \pm 6$  nm. To determine how many antibodies are attached to GNP surface, we have synthesized Cy3 dye attached anti-spike antibody conjugated GNP. After separation of the Cy3 dye attached antibody conjugated GNPs from unconjugated molecules, we have added 10  $\mu\text{M}$  potassium cyanide to oxidize the GNP. After that, from the fluorescence data we have estimated that about 10 ng/mL antibodies are attached on GNP.

Fourier transform infrared (FTIR) spectra from anti-spike-antibody attached gold nanoparticle reported in Figure S2E, shows the presence of Amide-A, Amide-I, Amide-II and Amide-II bands, which indicates that anti-spike-antibody are attached on gold nanoparticle surface. Inserted picture in Figure S1C shows the color of freshly prepared antibody GNPs is pink. Figure 2D shows the absorption spectra of antibody attached gold nanoparticle, which shows  $\lambda_{\text{max}}$  for antibody attached gold nanoparticle is  $\sim 522$  nm which indicates that after attaching with

antibody, the optical spectrum for GNPs remains almost the same.

**Table 1: Size of GNP at different coating conditions, measured by dynamic light scattering technique. Table also reports how the size of anti-spike antibody attached gold nanoparticle varies in the presence of different amount of COVID-19 antigen via aggregation.**

System	Size measured by DLS
Citrate coated GNP	$15 \pm 2$ nm
PEG coated GNP	$18 \pm 4$ nm
Antibody coated GNP	$27 \pm 6$ nm
Antibody attached GNP (1.3 nM) with 1 pg/mL antigen	$60 \pm 30$ nm
Antibody attached GNP (1.3 nM) with 100 pg/mL antigen	$120 \pm 60$ nm
Antibody attached GNP (1.3 nM) with 500 pg/mL antigen	$200 \pm 80$ nm
Antibody attached GNP (1.3 nM) with 1 ng/mL antigen	$700 \pm 300$ nm
Antibody attached GNP (1.3 nM) with 5 ng/mL antigen	$900 \pm 300$ nm

The X-Ray diffraction (XRD) spectra from antibody attached gold nanoparticle as reported in Figure S2D shows (111), (200), (220) and (311) diffraction peaks, which indicate that the crystal pattern remains the same after conjugation with antibody.

### Surface Enhanced Raman Spectroscopy using spike-antibody attached gold nanoparticle

For the detection of COVID-19 antigen and virus using SERS, we have used our developed portable Raman spectrometer with laser excitation of 670 nm <sup>22-24,26-27</sup>. In our design we have used InPhotonics 670 nm Raman fiber optic probe for excitation and data collection. For SERS signal collections, we have used miniaturized QE65000 Scientific-grade Spectrometer from Ocean Optics <sup>22-24,26-27</sup>. All SERS spectra has been taken on drop-casted dried glass slide. For Raman data collection we have used 10-second acquisition time and 5-scan averaging, so that we could achieve very good signal-to-noise ratio <sup>22-24,26-27</sup>.

### SARS-CoV-2 pseudotype particles

The Pseudo SARS-CoV-2 (Cat #C1110G) was purchased from Montana Molecular, Bozeman, Montana 59715. The HEK293T cells (ATCC # CRL3216) plated in twelve well tissue culture dishes were infected with the pseudotyped virus with a dilution range of  $10^2$  to  $10^7$  and virus titers were calculated by counting the green fluorescent protein (GFP) positive cells under a fluorescent microscope <sup>36-38</sup>.

### Virus inhibition assays

HEK293T cells (ATCC # CRL3216) were plated on a 96-well plate in complete media (DMEM + 10% FBS) and incubated under normal growth conditions (5% CO<sub>2</sub> and 37°C, protected from light) for 12-24 hours <sup>36-38</sup>. These HEK293T cells express low levels of ACE2 receptor that is sufficient for SARS-CoV-2 entry. Dilutions of test nanoparticles were made in DMEM with an end volume of 100  $\mu\text{L}$  each <sup>36-38</sup>. The pseudovirus stock (2.5  $\mu\text{L}$  of the  $2 \times 10^{10}$  units/ml stock) was mixed with the diluted



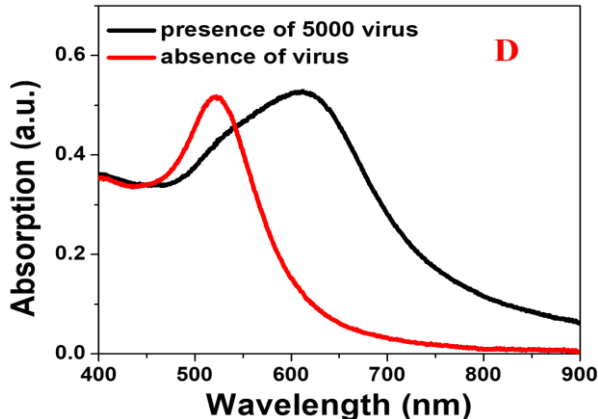
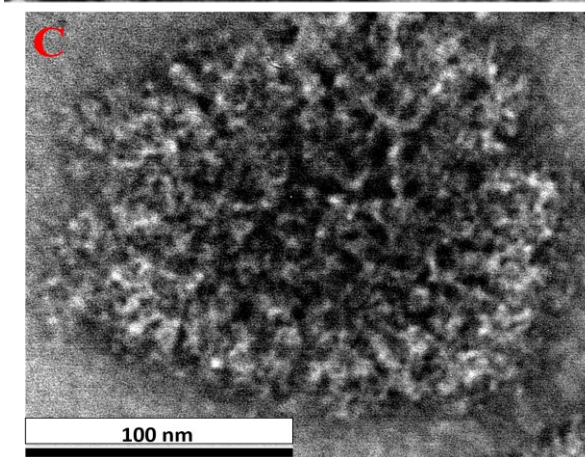
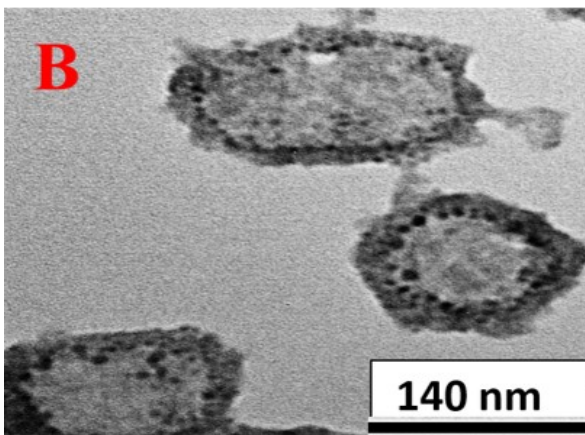
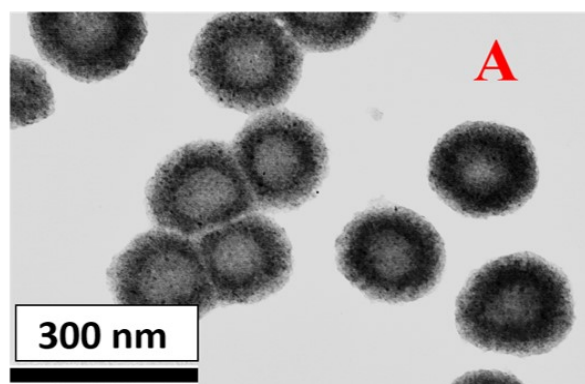
nanoparticles and incubated for 1 h at 37°C, then laid over HEK293T cells plated in the 96-well tissue culture dishes, along with 0.6  $\mu$ L of the 500 nM Sodium Butyrate (to give a final concentration of 2mM). Plates were incubated at 37°C and 5% CO<sub>2</sub> for 48 h. Cells were fixed in 3.7% formaldehyde and the assay was read on Cytation 5 automated fluorescent microscope (BioTek Instruments, Inc., Winooski, VT, USA)<sup>36-38</sup>.

## Results and Discussion

### Naked eye colorimetric diagnosis of COVID-19 antigen using anti-spike antibody attached gold nanoparticle

Antigen tests are used in the clinics for diagnosis different virus infection and now FDA has granted rapid antigen tests that can identify SARS-CoV-2<sup>2</sup>. Here our experimental data indicate that naked eye colorimetric diagnosis of COVID-19 antigens can be performed within 5 minutes using anti-spike antibody attached gold nanoparticle. As shown in Figure S1D in the supporting information, naked eye colorimetric diagnosis of COVID-19 antigens using antibody attached GNPs are based on the fact that in the presence of COVID-19 antigen, due to the antigen-antibody interaction, antibody attached GNPs aggregates, as shown in Figures S2A-C in the supporting information. As a result, as reported in Figures 1A-1C, we have observed the color change of the suspension of antibody attached GNPs from purple to bluish, which is due to the surface plasmon coupling between antibody attached GNPs. Reported TEM data in Figures S2A-2C and DLS data in Table 1 shows that as we increase the amount of COVID-19 antigen, the size of anti-spike antibody attached gold nanoparticle increases tremendously due to the aggregation. As we and others have reported before, when the interparticle distances are  $\sim 2.5$  times lower than diameter of the nanoparticles, the aggregation of gold nanoparticles will induce the coupling of the plasmon modes very strongly, which will induce a red shift of the absorption spectra<sup>28-33</sup>. Absorption spectra reported in Figure 1D shows red shift of absorption from 520 to 600 nm for aggregated antibody attached GNP. Reported absorption spectra also indicates the broadening of the plasmon resonance peak after aggregation of antibody attached GNP, which can be due to the longitudinal resonance.

To determine the sensitivity of naked eye colorimetric assay for the identification of COVID-19 antigen using antibody attached GNPs, we have performed antigen concentration dependent study starting from 1 pg/mL to 10000 pg/mL COVID-19 antigen. As shown in Figure 1B, naked eye colorimetric assay can be used for the diagnosis of minimum concentration of 1000pg/mL or 1ng/mL antigen. Next, we have determined the selectivity of the naked eye colorimetric assay for the identification of COVID-19 antigen using antibody attached GNPs. Since COVID-19, severe acute respiratory syndrome coronaviruses (SARS-CoV) and Middle East respiratory syndrome coronavirus (MERS-CoV) are caused by coronaviruses, we have also performed the same experiment for SARS-CoV virus antigen and MERS-CoV antigen separately using anti-spike antibody attached gold nanoparticle. As shown in Figure 1C, we have not observed any colorimetric change even when 5 ng/mL SARS-CoV virus antigen or MERS-CoV antigen was added to the pink color solution of anti-spike antibody attached gold nanoparticle. The above reported data clearly show that the antibody attached GNPs based naked eye colorimetric assay is highly selective for COVID-19 spike-antigen test.



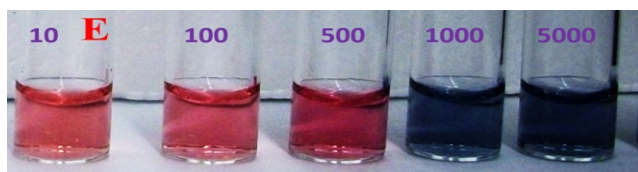


**Figure 2:** A) TEM shows the morphology of Pseudo SARS-CoV-2, which we have used for virus diagnosis. B) TEM shows the morphology of antibody attached GNPs conjugated Pseudo SARS-CoV-2 when we have used 20 pM gold nanoparticle. C) TEM shows the morphology of anti-spike antibody attached gold nanoparticle conjugated Pseudo SARS-CoV-2 when we have used 800 pM gold nanoparticle. D) Figure shows how the absorption spectra from antibody attached GNPs varies in the presence and absence of Pseudo SARS-CoV-2. E) Picture shows how the color of antibody attached GNPs changes in the presence of different amount of Pseudo SARS-CoV-2 (number of virus particles/mL).

### Naked eye colorimetric diagnosis of Pseudo SARS-CoV-2 using antibody attached GNPs

As we have discussed before, since SARS-CoV-2 is a biosafety-level-3 (BSL-3) virus, we have used a BSL-2, Pseudo SARS-CoV-2 with spike (S) protein as a model system for our diagnosis experiment<sup>36-37</sup>. As shown in Figures S1E and 2E, naked eye colorimetric diagnosis of Pseudo SARS-CoV-2 using antibody attached GNPs are based on the fact that in the presence of Pseudo SARS-CoV-2, due to the virus spike protein-antibody interaction, antibody attached GNPs aggregate on the surface of virus as shown in Figures 2A-C. Since the size of the Pseudo SARS-CoV-2 is around 120-160 nm, several antibody attached GNP can aggregate on the surface of virus. TEM reported in Figure 2C shows that as we increase the concentration of antibody attached GNP, due to the virus spike protein-antibody interaction, antibody attached GNPs aggregate and it covers the surface of whole viruses. As a result, as reported in Figure 2E, we have observed the color change of the suspension of antibody attached GNP from purple to bluish, which is due to the surface plasmon coupling between antibody attached GNP. Our reported naked eye colorimetric diagnosis of Pseudo SARS-CoV-2 using antibody attached GNP is very quick and it takes less than 5 minutes to get the results. Absorption spectra reported in Figure 2D shows red shift of absorption from 520 to 640 nm for aggregated antibody attached GNPs in the presence of Pseudo SARS-CoV-2.

To determine the sensitivity of naked eye colorimetric assay for the identification of Pseudo SARS-CoV-2 using antibody attached GNPs, we have performed Pseudo SARS-CoV-2 concentration dependent study starting from 10 virus particles/mL to 5000 virus particles/mL. As shown in Figure 2E, naked eye colorimetric assay can be used for the diagnosis of minimum concentration of 1000 virus particles/mL of Pseudo SARS-CoV-2. Our reported naked eye colorimetric assay for SARS virus detection exhibits slightly higher sensitivity than the antibody attached GNP based influenza A virus detection as reported by Liu et. al.<sup>40</sup>.

### Highly Sensitive SERS diagnosis of COVID-19 antigen and Pseudo SARS-CoV-2 using antibody attached GNPs

Although naked eye colorimetric assay is capable for the identification of COVID-19 antigen and Pseudo SARS-CoV-2

within 5 minutes time period, the sensitivity is low. To enhance the sensitivity significantly, we have employed SERS technique for the diagnosis of COVID-19 antigen and Pseudo SARS-CoV-2. As shown in Figure 3A, for rapid and highly sensitive identification via SERS, we have used 4-aminothiophenol as reporter molecules, which are attached to gold nanoparticle via Au-S bond. Synthesis details has been reported in the supporting information.

Figure 3B shows the SERS spectra from only anti-spike antibody (10 ng/mL) attached GNP (1.3 nM), only 4-aminothiophenol (300 nM) attached GNP (1.3 nM) and antibody (10 ng/mL) as well as 4-aminothiophenol (300 nM) attached gold nanoparticle (1.3 nM). As reported in Figure 4B, in the absence of 4-aminothiophenol Raman reporter, we have not observed any Raman signal, which clearly shows that the observed Raman spectra is mainly due to the presence of 4-aminothiophenol Raman reporter. Reported Raman spectra in Figure 3B from anti-spike antibody and 4-aminothiophenol attached gold nanoparticle show several Raman peaks due to the  $a_1$  vibrational modes and these are  $\nu(\text{C}-\text{C} + \text{NH}_2 \text{ bend})$  at  $\sim 1590 \text{ cm}^{-1}$  and  $\nu[\nu(\text{C}-\text{C}) + \delta(\text{C}-\text{H})]$  at  $\sim 1078 \text{ cm}^{-1}$ <sup>17-27</sup>. Similarly, we have also observed several  $b_2$  mode Raman peaks from the anti-spike antibody and 4-aminothiophenol attached gold nanoparticle as reported in Figure 3B and these are CC stretch in Ph ring +  $\text{NH}_2$  rock at  $\sim 1435 \text{ cm}^{-1}$  and  $\nu(\text{C}-\text{N}) + \nu(\text{C}-\text{S}) + \gamma(\text{CCC})$  vibrational modes at  $464 \text{ cm}^{-1}$ <sup>17-27</sup>.

Our SERS based diagnosis of COVID-19 antigens using antibody attached GNPs are based on the fact that in the presence of COVID-19 antigen, due to the antigen-antibody interaction, antibody attached GNPs aggregates and form several “hot spots” as shown in Figures S2A-C in the supporting information. It is now well documented that “hot spots” formation is very important factor to provide extraordinary enhancements in SERS, due to the strong light-matter interaction via plasmon-excitation coupling<sup>17-27</sup>. As reported in Figure 3C, very strong SERS signals from anti-spike antibody and 4-aminothiophenol attached gold nanoparticle are observed in the presence of COVID-19 Spike Recombinant Antigen and it is due to the formation of huge amounts of electromagnetic “hotspots”, which enhances Raman intensity by several orders of magnitude via light-matter and matter-matter interactions<sup>17-27</sup>.

To understand better how “hot spot” formation enhances SERS signal enormously, we have performed the finite-difference time-domain (FDTD) simulation<sup>22-24,42-43</sup>. Theoretical details have been reported before by our group and other groups<sup>22-24,26-27,42-43</sup>. For the simulation, we have used 20 nm spherical gold nanoparticle, 670 nm wavelength, 0.001 nm mesh resolution, and 4000 fs time<sup>22-24,26-27</sup>. Figure 4H shows how the square of field enhancement ( $|E|^2$ ) varies with distance for nanoparticles. FDTD simulation data reported in Figure 3H indicates that more than 2 orders of magnitude higher field enhancement in “hot spot” position when gold nanoparticles formed aggregates. As we and others have reported before, Raman enhancement is proportional to  $|E|^4$ <sup>22-24,26-27,42-43</sup> and as a result, reported FDTD simulation data indicate that there is a possibility of 4 orders of magnitude Raman enhancement in “hot spot” position, when gold nanoparticles formed aggregates.

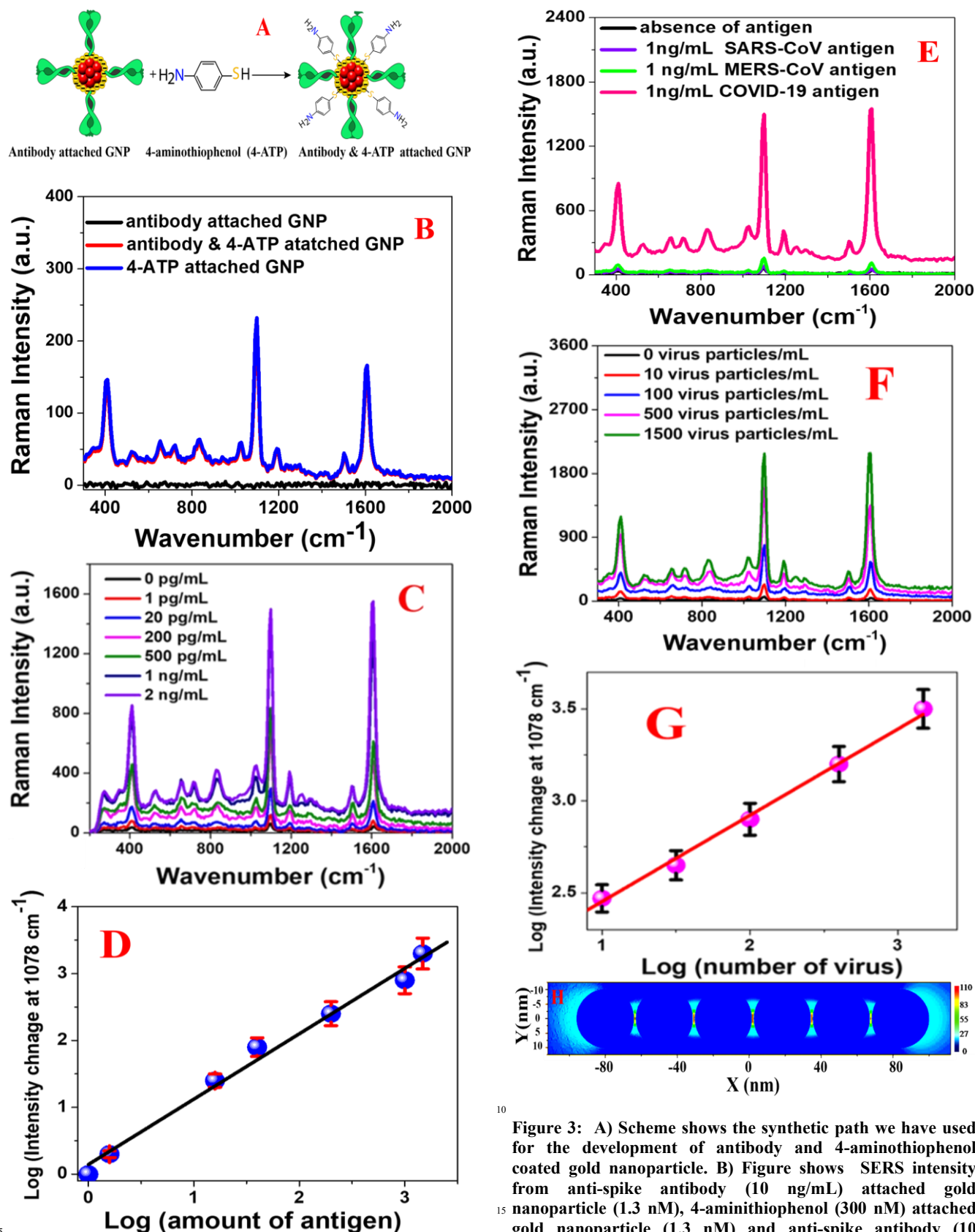


Figure 3: A) Scheme shows the synthetic path we have used for the development of antibody and 4-aminothiophenol coated gold nanoparticle. B) Figure shows SERS intensity from anti-spike antibody (10 ng/mL) attached gold nanoparticle (1.3 nM), 4-aminithiophenol (300 nM) attached gold nanoparticle (1.3 nM) and anti-spike antibody (10 ng/mL) as well as 4-aminithiophenol (300 nM) attached gold nanoparticle (1.3 nM). C) Figure shows how the SERS intensity from anti-spike antibody and 4-aminithiophenol attached gold nanoparticle varies in the presence of different



concentrations of COVID-19 antigen (COVID-19 Spike Recombinant Antigen). D) Plot shows how the Raman intensity change at  $1078\text{ cm}^{-1}$  from anti-spike antibody and 4-aminothiophenol attached gold nanoparticle varies with the concentration of COVID-19 Antigen (0 pg/mL to 2 ng/mL). E) Figure shows how the SERS intensity from anti-spike antibody and 4-aminothiophenol attached gold nanoparticle varies in the presence of different amount of Pseudo SARS-CoV-2 (number of virus particles/mL). G) Plot shows how Raman intensity change at  $1078\text{ cm}^{-1}$  from anti-spike antibody and 4-aminothiophenol attached gold nanoparticle varies with the concentration of Pseudo SARS-CoV-2 (number of virus particles/mL). H) FDTD simulation data show how the  $(|E|^2)$  profile varies with the increase of number of gold nanoparticles in aggregates.

Due to the above fact we have observed huge Raman signal enhancement in the presence of COVID-19 antigen. To determine the sensitivity of SERS assay for the identification of COVID-19 antigen using anti-spike antibody and 4-aminothiophenol attached gold nanoparticle, we have performed antigen concentration dependent study starting from 1 pg/mL to 2000 pg/mL COVID-19 antigen. As shown in Figure 3C, SERS assay can be used for the diagnosis of minimum concentration of 1pg/mL antigen, where we have observed more than 2 times of increment of the Raman signal. Figure 3D shows how the Raman signal at  $1078\text{ cm}^{-1}$  from anti-spike antibody and 4-aminothiophenol attached gold nanoparticle varies with the concentration of COVID-19 antigen.

To determine the limit of detection (LOD), we have used the following equation<sup>22-24</sup>.

$$\text{LOD} = 3\sigma/S \quad (1)$$

where,  $\sigma$  is the standard deviation of the blank and  $S$  is the slope of the calibration curve. For the determination of standard deviation of blank, we have used the baseline noise. Using the concentration-dependent linear curve reported in Figure 3D, we have estimated the LOD to be  $\sim 4\text{ pg/mL}$  for SERS assay using COVID-19 antigen. Next, we have determined the selectivity of the SERS assay for the identification of COVID-19 antigen using anti-spike antibody and 4-aminothiophenol attached gold nanoparticle. For this purpose, we have also performed the same SERS experiment for SARS-CoV virus antigen and MERS-CoV antigen separately using anti-spike antibody and 4-aminothiophenol attached gold nanoparticle. As shown in Figure 3E, we have not observed any SERS intensity change even when 1 ng/mL SARS-CoV antigen or MERS-CoV antigen was added to anti-spike antibody and 4-aminothiophenol attached gold nanoparticle. The above reported data clearly shows that antibody attached GNP-based SERS is highly selective for COVID-19 spike antigen test.

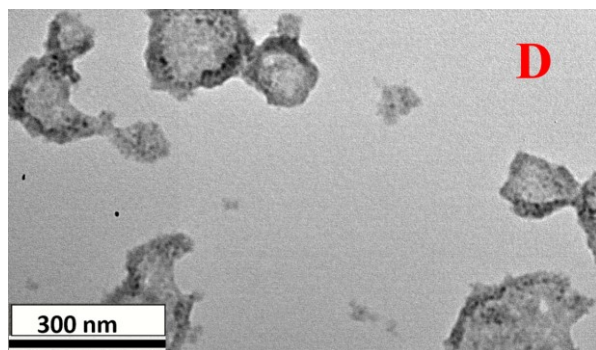
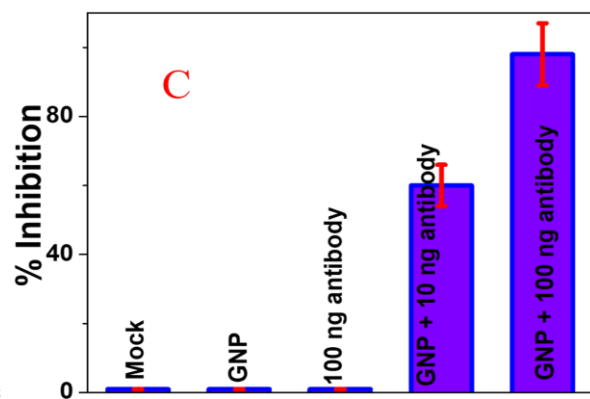
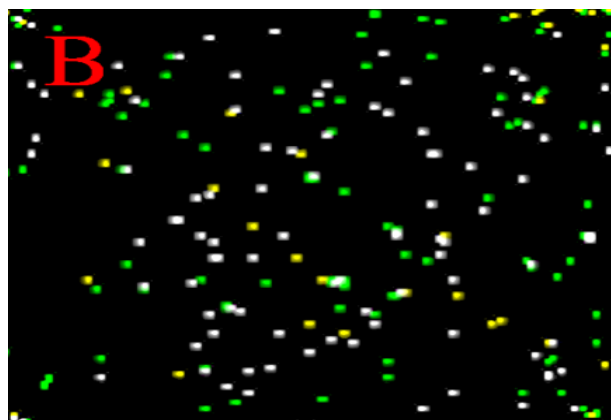
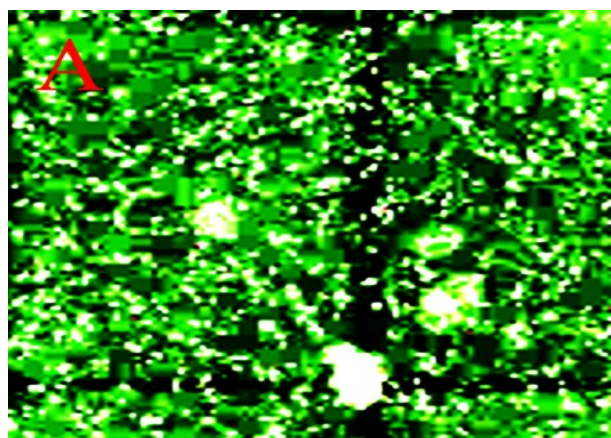
Our SERS based diagnosis of Pseudo SARS-CoV-2 using anti-spike antibody and 4-aminothiophenol attached gold nanoparticles are based on the fact that in the presence of Pseudo SARS-CoV-2, due to the virus spike protein-antibody interaction, anti-spike antibody and 4-aminothiophenol attached gold nanoparticles aggregates on the surface of virus as shown in Figures 2B-C. Since the size of the Pseudo SARS-CoV-2 is around 120-150 nm, several anti-spike antibody and 4-

aminothiophenol attached gold nanoparticles can aggregate on the surface of virus and form several "hot spots". As a result, as reported in Figure 3F, we have observed huge SERS intensity change, which is due to the surface plasmon coupling between anti-spike antibody and 4-aminothiophenol attached gold nanoparticles. Our reported SERS diagnosis of Pseudo SARS-CoV-2 using anti-spike antibody and 4-aminothiophenol attached gold nanoparticles is very quick which takes less than 5 minutes to get the results.

To determine the sensitivity of SERS assay for the identification of Pseudo SARS-CoV-2 using anti-spike antibody and 4-aminothiophenol attached gold nanoparticle, we have performed virus concentration dependent study starting from 10 viruses to 1500 Pseudo SARS-CoV-2. As shown in Figure 3F, SERS assay can be used for the diagnosis of minimum concentration of 10 virus particles/mL, where we have observed more than 2 times of increment of the Raman signal. Figure 3G shows how the Raman signal at  $1078\text{ cm}^{-1}$  from anti-spike antibody and 4-aminothiophenol attached gold nanoparticle vary with the concentration of Pseudo SARS-CoV-2. Using the Equation 1 and the concentration-dependent linear curve reported in Figure 3G, we have estimated the LOD to be  $\sim 18$  virus particles/mL for SERS assay using pseudo SARS-CoV-2. Reported SERS detection assay is comparable with the Abbott Real Time SARS-CoV-2 RT-PCR assay (40 copies/mL)<sup>44</sup>.

### Inhibition of Pseudo SARS-CoV-2 using anti-spike antibody attached gold nanoparticle

It is now well documented that SARS-CoV-2 fusion with host cell membranes proceed through interactions between spike proteins of virus and ACE2 receptor on the surface of human cells<sup>5-16,34-41</sup>. To find out whether anti-spike antibody attached gold nanoparticle has the capability to block the viral entry into cells, we have used Pseudo SARS-CoV-2 (#C1110G, Montano Molecular, Bozeman, MT) as the model virus<sup>36-38</sup>. For our inhibition experiment we have used HEK293T cells which express ACE2 by which SARS-CoV-2 entry in human cells are determined<sup>36-38</sup>. As reported in Figures 4A-4C, anti-spike antibody attached gold nanoparticle blocks viral replication and virus spread in HEK293T cells. Reported data show that the inhibition efficiency was 100% for 100 ng/mL anti-spike antibody attached gold nanoparticle. On the other hand, for 10 ng/mL anti-spike antibody attached GNP, the inhibition efficiency was 60%. Similarly, reported experimental data indicate that the inhibition efficiency for PEG coated GNP and 100 ng/mL antibody only was very low, which is less than 1%. Although for the design of anti-spike-antibody we have used 100 ng/mL antibody, reported data indicate 100% inhibition efficiency in the presence of 100 ng/mL anti-spike-antibody attached gold nanoparticle, which may be due to the fact that antibody attached gold nanoparticles bind to Pseudo SARS-CoV-2, thereby inhibiting the virus from binding to the cell receptor<sup>14,34-41</sup>. As a result, it does not allow the virus from infecting the targeted cells<sup>34-41</sup>. As reported in Figure 4D, antibody attached GNPs have the capability to break the lipid membrane of Pseudo SARS-CoV-2, so that the virus particle collapses<sup>34-41</sup>. As we and others have reported before, gold nanoparticles suppress viral infection by selectively cleaving disulfide bonds, which blocks membrane fusion and viral entry to the host cell<sup>14,34-35,38-41</sup>. We believe that all the above discussed mechanisms are responsible for 100% inhibition efficiency observed using the anti-spike-antibody attached gold nanoparticle.



cells in the presence of 10 ng/mL anti-spike antibody. C) Plot shows how inhibition efficiency of SARS-CoV-2 pseudovirus green fluorescent protein (GFP) expression in infected HEK293T cells vary in the presence of buffer (Mock), gold nano particle (GNP), anti-spike antibody and anti-spike antibody attached gold nanoparticle. D) TEM image shows that possibly 100 ng/mL anti-spike antibody attached gold nanoparticle break the lipid membrane of pseudo SARS-CoV-2.

## Conclusions

We have developed novel anti-spike antibody attached gold nanoparticle for rapid diagnosis and inhibition of virus. Reported data demonstrated that antibody attached GNPs can be used for the naked eye detection of specific COVID-19 viral antigen or of Pseudo SARS-CoV-2 via simple colorimetric change. Experimental data show that anti-spike antibody attached gold nanoparticle-based sensing of COVID-19 viral antigen or virus is very fast and can be detected within 5 minutes time period. Reported data show that naked eye assay allows to determine the presence of antigen or virus even at the concentration of 1ng/mL for COVID-19 antigen and 1000 virus particles/mL for Pseudo SARS-CoV-2. We have also demonstrated that using anti-spike antibody and 4-aminothiophenol attached gold nanoparticle-based SERS, one can diagnose COVID-19 viral antigen or virus at very low concentrations within 5 minutes of time period. Using portable Raman analyzer, reported data show that antibody and 4-aminothiophenol attached gold nanoparticle-based SERS probe has the capability to detect COVID-19 antigen even at the concentration of 4 pg/mL and virus at the concentration of 18 virus particles/mL. Reported finite-difference time-domain (FDTD) simulation data indicate that 4 orders of magnitude Raman enhancement occurs in “hot spot” position, when gold nanoparticles formed aggregates.

Using HEK293T cells, which express angiotensin-converting enzyme 2 (ACE2) by which SARS-CoV-2 entry in human cells, we demonstrated that anti-spike antibody attached gold nanoparticle have the capability to control the virus infection. Reported data show that the inhibition efficiency is 100% for anti-spike antibody attached gold nanoparticle. On the other hand, for only GNP, the inhibition efficiency is only around 1% and for 100 ng/mL antibody, the inhibition efficiency is less than 1%. Reported data indicate 100% inhibition efficiency in the presence of anti-spike-antibody attached gold nanoparticle, which may be due to the fact that antibody attached gold nanoparticles bind to Pseudo SARS-CoV-2, thereby inhibiting the virus from binding to the cell receptor. Reported data show that antibody attached GNPs block viral replication and virus spread in HEK293T cells. It also destroys the virus lipid membrane.

## Conflict of interest

There are no conflicts of interest to declare

## Acknowledgements

Dr. Ray thanks NSF-RAPID grant # DMR-2030439 and NSF-PREM grant # DMR-1826886, for their generous funding. We also thank NIH-NIMHD grant # 1U54MD015929-01 for bioimaging core facility. Dr. Tandon is supported by NASA award (80NSSC19K1603) and COVID-19 funds from the University of Mississippi Medical Center.



## Notes and References

1. <https://www.who.int/health-topics/coronavirus> (accessed 11/24/2020)
2. <https://www.cdc.gov/coronavirus/2019-ncov/hcp/nursing-homes-antigen-testing.html> (accessed 11/24/2020)
3. D. Wrapp, N. Wang, K. S. Corbett, J. A. Goldsmith, C. L. Hsieh, O. Abiona, B. S. Graham, J. S. McLellan, *Science* 2020, **367**, 1260–1263
4. C. Wang, P. W. Horby, F. G. Hayden, G. F. Gao, *Lancet* 2020, **395**, 470–473
5. J. P. Broughton, X. Deng, G. Yu, C. L. Fasching, V. Servellita, J. Singh, X. Miao, J. A. Streithorst, A. Granados, A. Sotomayor-Gonzalez, K. Zorn, A. Gopez, E. Hsu, W. Gu, S. Miller, C. Y. Pan, H. Guevara, D. A. Wadford, J. S. Chen and C. Y. Chiu, *Nat. Biotechnol.*, 2020, **38**, 870–874
6. X. Ou, Y. Liu, X. Lei, P. Li, D. Mi, L. Ren, L. Guo, R. Guo, T. Chen, J. Hu, Z. Xiang, Z. Mu, X. Chen, J. Chen, K. Hu, Q. Jin, J. Wang and Z. Qian, *Nat. Commun.*, 2020, **11**, 1620
7. M. Gandhi, D. S. Yokoe, D. V. Havlir, *N. Engl. J. Med.* 2020, **382**, 2158–2160
8. F. Krammer and V. Simon, *Science*, 2020, **368**, 1060–1061
9. B. Udugama, P. Kadhiresan, H. N. Kozlowski, A. Malekjahani, M. Osborne, V. Y. C. Li, H. Chen, S. Mubareka, J. B. Gubbay and W. C. W. Chan, *ACS Nano*, 2020, **14**, 3822–3835
10. R. A. Moreira, M. Chwastyk, J. L. Baker, H. V. Guzman, A. B. Poma, *Nanoscale*, 2020, **12**, 16409–16413
11. Z. Chen, Z. Zhang, X. Zhai, Y. Li, L. Lin, H. Zhao, L. Bian, P. Li, L. Yu, Y. Wu, G. Lin, *Anal. Chem.* 2020, **92**, 7226–7231
12. G. Qiu, Z. Gai, Y. Tao, J. Schmitt, G. A. Kullak-Ublick, J. Wang, J., *ACS Nano* 2020, **14**, 5268–5277
13. P. Moitra, M. Alafeef, K. Dighe, M. B. Frieman, D. Pan, *ACS Nano* 2020, **14**, 7617–7627
14. B. D. Ventura, M. Cennamo, A. Minopoli, R. Campanile, S. B. Censi, D. Terracciano, G. Portella and R. Velotta, *ACS Sens.* 2020, **5**, 3043–3048
15. G. Seo, G. Lee, M. J. Kim, S. H. Baek, M. Choi, K. B. Ku, C. S. Lee, S. Jun, D. Park, S. J. Kim, J. O. Lee, B. T. Kim, E. C. Park, S. Kim, S., *ACS Nano* 2020, **14**, 5135–5142
16. M. Alafeef, K. Dighe, P. Moitra, D. Pan, D.; *ACS Nano* 2020, Article ASAP
17. R. Liu, L. He, Y. Hu, Z. Luo, J. Zhang, *Chem. Sci.*, 2020, **11**, 12157–12164
18. C. Zong, M. Xu, L. J. Xu, T. Wei, X. Ma, X. S. Zheng, R. Hu, B. Ren., *Chem. Rev.* 2018, **118**, 4946–4980
19. S. Y. Ding, E. M. You, Z. Q. Tian, M. Moskovits, M. *Chem. Soc. Rev.* 2017, **46**, 4042–4076
20. H. Chen, A. Das, L. Bi, N. Choi, J. Moon, Y. Wu, S. Park and J. Choo, *Nanoscale*, 2020, **12**, 21560–21570
21. S. Rodal-Cedeira, A. Vázquez-Arias, G. Bodelón, A. Skorikov, S. Núñez-Sánchez, S. Laporta, L. Polavarapu, S. Bals, L. M. Liz-Marzán, J. Pérez-Juste, L. Pastoriza-Santos, *ACS Nano* 2020, Article ASAP.
22. A. Pramanik, J. Mayer, S. Patibandla, K. Gates, Y. Gao, D. Davis, R. Seshadri, P. C. Ray, *ACS Omega* 2020, **5**, 27, 16602–16611
23. M. A. Paul, Z. Fan, S. S. Sinha, Y. Shi, L. Le, F. Bai, P. C. Ray, *J. Phys. Chem. C* 2015, **119**, 23669–23675
24. S. S. Sinha, S. Jones, A. Pramanik, P. C. Ray, *Acc. Chem. Res.*, 2016, **49**, 2725–2735
25. D. Cialla-May, X. S. Zheng, K. Weber, J. Popp, J. *Chem. Soc. Rev.* 2017, **46**, 3945–3961
26. A. K. Singh, S. A. Khan, Z. Fan, T. Demeritte, D. Senapati, R. Kanchanapally, P. C. Ray, *J. Am. Chem. Soc.* 2012, **134**, 8662–8666
27. S. Jones, S. S. Sinha, A. Pramanik, P. C. Ray, *Nanoscale* 2016, **8**, 18301–18308
28. W. Lu, S. R. Arumugam, D. Senapati, A. K. Singh, T. Arbleshi, S. A. Khan, H. Yu, P. C. Ray, *ACS Nano*, 2010, **4**, 1739–1749
29. S. Wang, A. K. Ding, D. Senapati, A. Neely, H. Yu, P. C. Ray, *Chem. A Eur. J.*, 2010, **16**, 5600–5606.
30. J. R. Kalluti, T. Arbnesi, S. A. Khan, A. Neely, B. Varsili, M. Washington, S. McAfee, B. Robinson, A. K. Singh, D. Senapati, P. C. Ray, *Angew. Chem. Int. Ed.* 2009, **48**, 51, 9668–9671
31. F. Tian, J. Zhou, B. Jiao, Y. He, *Nanoscale*, 2019, **11**, 9547–9555
32. S. Xu, W. Ouyang, P. Xie, Y. Lin, B. Qiu, Z. Lin, G. Chen, L. Guo, L. *Anal. Chem.* 2017, **89**, 1617–1623
33. H. Kim, M. Park, J. Hwang, J. H. Kim, D. R. Chung, K. S. Lee, M. Kang, M. *ACS Sens.* 2019, **4**, 1306–1312
34. R. Kumar, P. C. Ray, D. Datta, G. P. Bansal, E. Angov N. Kumar *Vaccine*. 2015, **33**, 5064–71
35. M. B. DeRussy, M. A. Aylward, Z. Fan, P. C. Ray, R. Tandon. R.; *Scientific Reports* 2014, **4**, Article number: 5550, doi:10.1038/srep05550
36. W. Jin, W. Zhang, D. Mitra, M. G. McCandless, P. Sharma, R. Tandon, F. Zhang, R. J. Linhardt, *Int. J. Biol. Macromol.*, 2020, **163**, 1649–1658
37. R. Tandon, D. Mitra, P. Sharma, M. G. McCandless, S. J. Stray, J. T. Bates, G. D. Marshall *Sci Rep.* 2020 **5**, 10, 19076.
38. R. Tandon, J. S. Sharp, F. Zhang, V. H. Pomin, N. M. Ashpole, D. Mitra, M. G. McCandless, W. Jin, H. Liu, P. Sharma, R. J. Linhardt *J Virol.* 2020 (ASAP Article)
39. T. Du, J. Zhang, C. Li, T. Song, P. Li, J. Liu, X. Du, X.; S. Wang, S.; *Bioconjugate Chem.* 2020, ASAP Article
40. Y. Liu, L. Zhang, W. Wei, H. Zhao, Z. Zhou, Y. Zhang, S. Liu, *Analyst*, 2015, **140**, 3989–3995.
41. X. Huang, M. Li, Y. Xu, J. Zhang, X. Meng, X. An, L. Sun, L. Guo, X. Shan, J. Ge, J. Chen, Y. Luo, H. Wu, H., Y. Zhang, Y.; Jiang, X. Ning, *ACS Appl. Mater. Interfaces* 2019, **11**, 19799–19807
42. J. Zhao, A. O. Pinchuk, J. M. McMahon, S. Li, L. K. Ausman, A. L. Atkinson, G. C. Schatz, *Acc. Chem. Res.* 2008, **41**, 1710–1720
43. M. W. Knight, N. S. King, L. Liu, H. O. Everitt, P. Nordlander, N. J. Halas, N. J. *ACS Nano* 2014, **8**, 834–840
44. <https://www.molecular.abbott/us/en/products/infectious-disease/RealTime-SARS-CoV-2-Assay>